

New Imaging Camera for the MAGIC-I Telescope

D. NAKAJIMA¹, D. FINK¹, J. HOSE¹, R. MIRZOYAN¹, D. PANEQUE¹, K. SAITO¹, T. SCHWEIZER¹, M. TESHIMA¹, T. TOYAMA¹, H. WETTESKIND¹ FOR THE MAGIC COLLABORATION.

¹ Max-Planck-Institut fuer Physics, Foehringer Ring 6, 80805 Munich

nakajima@mpp.mpg.de

Abstract: MAGIC is a system of two large imaging atmospheric Cherenkov telescopes located on the Roque de los Muchachos European North Observatory on the Canary island of La Palma at a height of 2200 m a.s.l.. The first telescope (MAGIC-I) has been operational since 2004 for scientific observation of very high energy gamma source candidates in the energy range of 55 GeV to 50 TeV. The second telescope (MAGIC-II) was installed at a distance of 85 m away from MAGIC-I in 2008. From the end of 2008, we started operating them together in stereoscopic mode. Both telescopes have a 17 m diameter reflective surface and a camera. The MAGIC-I camera consisted of 397 pixels that were based on 1 inch size photomultiplier tubes for the inner part of the camera and 180 pixels of 1.5 inch tubes for the outer part. The camera of MAGIC-II is composed of 1039 pixels of one inch super-bialkali photomultiplier tubes. In Summer 2012, aiming to make the system more homogeneous, we have upgraded the camera of MAGIC-I. The new camera has been built and tested intensively at Max-Planck-Institute for Physics in Munich and has been installed on site. The pixel structure of the new camera is the same as the one of MAGIC-II, while in the meantime the new photomultiplier tubes show an improved peak quantum efficiency. In addition, we have introduced some improvements in the design. Here we report the main features of the new MAGIC-I camera.

Keywords: MAGIC, Gamma-ray astronomy, Imaging Atmospheric Cherenkov Telescopes, Photomultipliers

1 Introduction

MAGIC (Major Atmospheric Gamma Imaging Cherenkov telescopes) consist of two 17 m diameter Imaging Atmospheric Cherenkov Telescopes (IACT) installed at a height of 2200 m a.s.l. on the Roque de los Muchachos European North Observatory on the Canary island of La Palma in Spain. The telescopes observe very high energy cosmic gamma rays in the energy range of 55 GeV to 50 TeV, accessing lowest energy threshold among any existing ground based gamma ray telescopes so far [1]. The first telescope, MAGIC-I, has been in operation since 2004. After the installation of the second telescope, MAGIC-II, in 2009, the two telescope system started stereoscopic observations which improves the energy and the angular resolution of the system. Both telescopes have a parabolic reflector with a diameter of 17 m and a camera composed of pixels based on photomultiplier tubes (PMTs). The cameras are mounted in the focal plane of the reflector and have a field-of-view (FoV) of ~ 3.5 degree in diameter. The camera of MAGIC-I was equipped with 397 inner and 180 outer pixels. The inner and outer part of pixels were based on PMTs respectively of type ET9116 (Electron Tubes Enterprises) with a diameter of 1 inch and a FoV of 0.1 degrees, and of type ET9117 (Electron Tubes Enterprises) with a diameter of 1.5 inch and a FoV of 0.2 degrees. The camera of MAGIC-II are equipped with 1039 pixels based on super-bialkali photomultiplier tubes, R10408 (Hamamatsu Photonics). The PMTs have a diameter of 1 inch which cover a FoV of 0.1 degrees. Those PMTs show a peak quantum efficiency (QE) of ~ 32 %.

After 9 years of operation of MAGIC-I telescope, we have exchanged the camera of MAGIC-I as a part of MAGIC upgrade [2]. The new MAGIC-I camera has the same pixel structure as MAIGIC-II which allowed us to

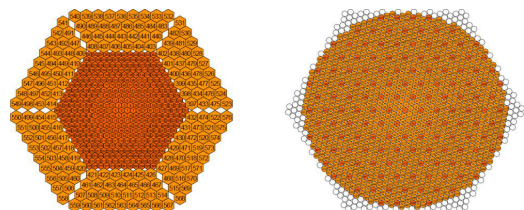


Fig. 1: Photograph of the camera (*top*) and the pixel structure of the old (*bottom-left*) and the new (*bottom-right*) MAGIC-I camera.

unify several subsystems for easier maintenance for the next future 5 to 10 years.

2 The camera

The photo of the new MAGIC-I camera is shown in Fig. 1 (top) as well as the pixel structure of the old and the new MAGIC-I cameras in Fig. 1 (bottom left) and (bottom right), respectively. The new camera has nearly circular shape with a FoV of ~ 3.5 degree. A group of 7 pixels are assembled together into one cluster. In total, the camera is equipped with 169 clusters. Among the 169 clusters, 127 are fully equipped with 7 pixels (colored in orange in Fig. 1 bottom-right), while 42 clusters located in the edge of the camera are partially equipped with several pixels (colored in white in Fig. 1 bottom-right). Fig. 2 shows a photo of a cluster and a PMT pixel. The analogue signals from the PMTs are converted into an optical pulse using Vertical Cavity Surface Emitting Laser diodes (VCSELs) and transmitted to the readout system in the counting house over 162 m of optical fibers. The VCSELs are operated at a wavelength of 850 nm. Each cluster has its own slow control processor (SCCP) which controls several parameters of PMTs such as the setting/reading of H.V., reading the anode DC current and temperature. The H.V. of the PMTs is produced by a Cockroft-Walton (CW) type DC-DC converter. Furthermore, a pulse generator is installed into each cluster, which allows us to inject a signal similar to the PMT pulses into the electronic chain. This feature can be used for technical studies of entire amplification chain even during the day, time when the H.V. is preferably not to be applied to the PMTs.

The clusters are inserted into a support frame in the camera, in which cooling water is continuously circulating in a closed loop. This system is operating under the control of a computer and provides temperature stability of the clusters. In the camera, two VME crates are installed to establish the communication between the camera and the central control system via optical PCI. All clusters are connected to the VME crates and their status are monitored at a rate of 10 Hz. All electronics in the camera are powered by several 5 V low-noise switching power supplies (Kniel) mounted from outside, in the bottom of the camera housing. The maximum power consumption is expected to be below 1 kW. On the front side of the camera, a Plexiglas window is attached in order to protect the PMT clusters from adverse weather conditions.

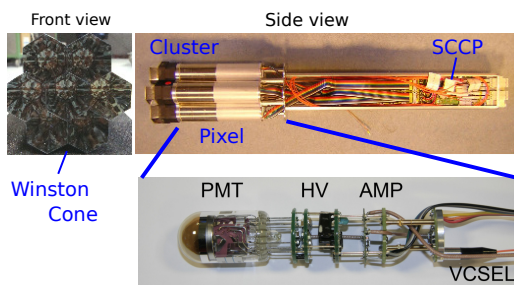


Fig. 2: Photograph of a cluster with 7 PMTs front view (top-left), side view (top-right) and a single pixel (bottom).

3 Evaluation of the PMTs

A pixel is equipped with a super-bialkali type PMT (R10408) from Hamamatsu Photonics. The PMT has a hemispherical photo-cathode with a diameter of 1 inch. The

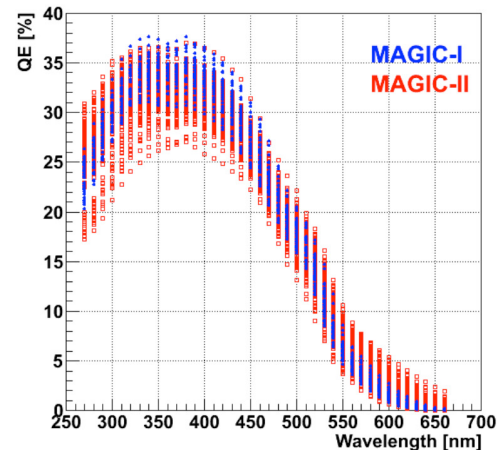


Fig. 3: Quantum efficiency of new PMTs (blue) as a function of wavelength compared with one of MAGIC-II PMTs (red).

PMTs are basically same as the one used in the MAGIC-II camera, but in the meantime the new PMTs show on average slightly higher peak QE of around 34 % compared to the MAGIC-II camera PMTs (~ 32 %). Fig. 3 shows the quantum efficiency of PMTs as a function of wavelength for the new MAGIC-I and MAGIC-II cameras. The PMT has 6 dynodes and the typical operational gain is $\sim 3 \times 10^4$. Each pixel has its own CW type DC-DC converter, which can provide a voltage of up to 1250 V, and an analogue signal processor front-end circuit which includes a preamplifier and a VCSEL. In front of the photo-cathode, a Winston-cone type light guide is attached in order to minimize the dead space between neighboring PMTs and to reduce background light coming from large angles.

All PMT clusters have been assembled at Max-Planck-Institute for Physics (MPI) in Munich. Performances and functionality of all clusters with PMTs have been checked in the laboratory at MPI by means of a fast pulsed laser (STV-01E from Soliton). The UV laser pulse (355 nm) is generated from the 3rd harmonic conversion from a passively Q-switched Nd:YAG. Its pulse width is ~ 700 ps and its energy is $1.2 \mu\text{J}$ at a maximum frequency of 2 kHz. A cluster was placed in a dark box (1000 mm \times 500 mm \times 500 mm) [3] and irradiated uniformly by the laser. In order to protect the setup from electromagnetic pickup noise, the inside of the dark box has been entirely coated with a copper silver fleece (Aaronia X-Dream plus) which screens the noise more than -80 dB up to a frequency of 10 GHz. The laser first crosses two optical filters, which are held in two 12 position filter wheels, allowing us to adjust the intensity of the laser. The laser pulses are then diffused uniformly by using an integration sphere made of Spectralon. In addition, one PMT is placed alongside of the cluster as a reference, which is used to monitor the system. A signal readout was performed based on a bank of CAEN FADCs with 300 MHz bandwidth and 2 GSample/s sampling rate. A typical pulse shape of a signal induced by the laser is shown in Fig. 4. The mean pulse width is 2.8 ns FWHM. For all clusters, 1) gain adjustment (flat-fielding), 2) linearity of the amplification chain, 3) single photo-electron response, 4) after pulses 5) dynamic range and 6) noise factor F are evaluated and characterized. All

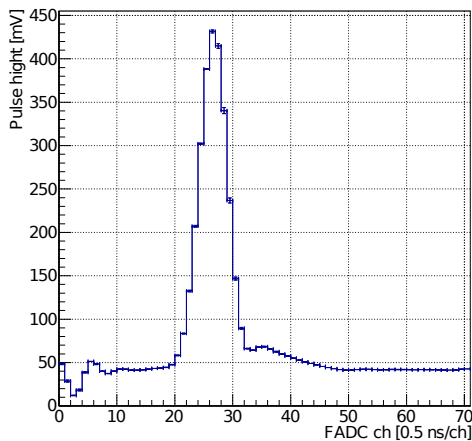


Fig. 4: Typical pulse shape of a PMT.

those measurements listed above and the control of filter wheels and the laser have been performed automatically by a LabView program.

4 Evaluation of the camera

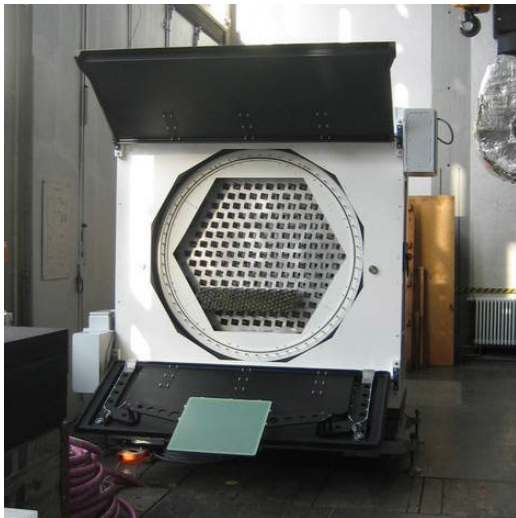


Fig. 5: Photograph of the new MAGIC-I camera assembled at MPI.

In advance to the installation, the camera was built up at MPI and its performance has been evaluated. A complete camera including all pixels, the cooling unit and the low voltage power supply were mounted. Fig. 5 shows a photograph of the construction when the clusters were being installed.

After the construction, a dark room made from wood ($\sim 8 \text{ m} \times 2.5 \text{ m} \times 2.5 \text{ m}$) was constructed around the camera. In the dark room, a calibrated laser driver was mounted at $\sim 6 \text{ m}$ away from the front plane of the camera. The calibrator is equipped with a laser head, two filter wheels and an integrating sphere. The laser head is a frequency tripled passively Q-Switched Nd:YAG laser operated at the third harmonic of 355 nm. Two rotating optical filter wheel are installed in the device which allow us to control the

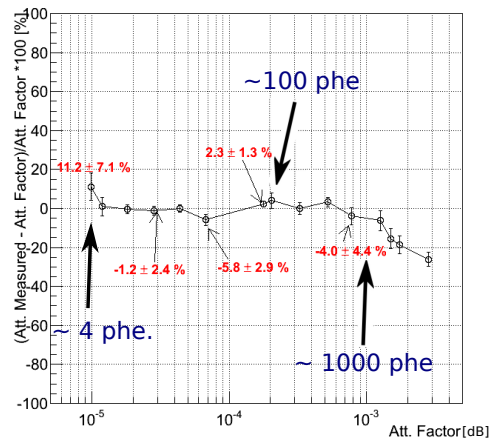


Fig. 6: A deviation of non-linearity of all 1039 pixels as a function of the attenuation factor of the laser light.

laser intensity. The pulse from it is randomly scattered in the integrating sphere and then the uniformly distributed light illuminates the entire camera plane homogeneously. The data acquisition was performed by a custom made multiplexed system with commercial 2 GSamples/s FADC (DC 282 from Acqiris). The system is the so-called MUX-FADC [4] and was a standard readout system for the MAGIC-I camera until September 2011 [2].

Fig. 6 shows a deviation of from non-linearity of amplification chains, from PMT to the readout, of all pixels. The horizontal axis show an attenuation factor of the filters located in front of the laser head, which have been measured in the lab in advance. The vertical axis shows a deviation of the measured light intensity from the real light intensity which is known from the optical density of the used filters. The error bars on the plot are standard deviations of the non-linearity for all 1039 pixels. The leftmost point corresponds to a laser intensity of about 4 photoelectrons (phe) at the camera plane. As can be seen in the figure, it has been found that the entire analogue signal chain has a good linearity ($\leq 10\%$) for the dynamic range from a few phe up to ≤ 1000 phe.

Possible cross-talk was evaluated by introducing a big signal in only one pixel. It was found that the maximum cross-talk to the neighboring pixels in the same cluster are on the order of 0.5%. Cross-talk to the neighboring pixel in the next cluster is found to be less than 0.2%.

The performance of the cooling system has been checked by mounting 12 bulbs with 1 kW total heat dissipation capacity in the camera. Temperature was measured by using sensors at 6 places in the camera. The test showed that the temperature can be stabilized to a precision of ± 1 degree after about 2 hours and kept stable. The long term (~ 33 hours) stability of the cooling system as well as of the signal chain has also been studied. Especially the VCSELs exhibit a temperature dependence, therefore it is important to keep their temperature stable. The test shows that the stability of the signal is better than 3%. It was found that there is a temperature gradient from the center of the camera to the edge up to 5 degrees due to the path of the pipes in the cooling plate and mostly self-radiation of the camera. However the small temperature gradient between clusters



Fig. 7: Installation of the new MAGIC-I camera

does not have a big impact as long as the temperature of each pixel is stable.

During the intense integration test, it was found that the VME crate in the camera induces a communication noise on pixels around the crate. For this reason, a VME silencer, made of Ferrite foil (Buerklin) and Copper foil, has been mounted on the VME bus connectors in between the crate and the modules. It reduces the noise by a factor ~ 5 . Based on this study, the VME silencer was also implemented in the MAGIC-II camera. However it has to be noted here that only the pixels close to the VME crate are affected. These are located in the outer rings of the camera and do not participate in the trigger decision.

5 Installation on site

In July 2012, the new MAGIC-I camera has been installed on site successfully (Fig. 7). The new camera has been commissioned in August 2012. We have repeated the same tests which had been done at MPI and confirmed its expected performance. Normal observation using the new camera has been started from November 2012 [1, 2].

Acknowledgment: We would like to thank the electronics and mechanics departments at MPI for their excellent work for production of clusters and camera installation

References

- [1] R. Mirzoyan *et al.* "Recent Highlights of MAGIC", these proceedings
- [2] D. Mazin *et al.* "Upgrade of the MAGIC telescopes", these proceedings
- [3] Toni Engelhardt, bachelor thesis (2011)
- [4] H. Bartko, F. Goebel, R. Mirzoyan, W. Pimpl and M. Teshima, Nuclear Instruments and Methods in Physics Research A 548 (2005) 464486